Experimental test of variable loads on a vertical-axis wind turbine

Brandetti, L.; De Tavernier, D.; Leblanc, B.; Ferreira, C.

DOI
10.1088/1742-6596/1618/3/032037

Publication date
2020

Document Version
Final published version

Published in
Journal of Physics: Conference Series

Experimental test of variable loads on a vertical-axis wind turbine

Experimental test of variable loads on a vertical-axis wind turbine

L Brandetti, D De Tavernier, B LeBlanc and C Ferreira
Delft University of Technology, Wind Energy, Kluyverweg 1, Delft, The Netherlands
E-mail: l.brandetti@tudelft.nl

Abstract. The paper presents an experimental study of applying variable loads on a vertical-axis wind turbine (VAWT). The experiment is conducted in an open-jet wind tunnel on a two-bladed Darrieus VAWT equipped with active individual blade pitch control. Variable loads are achieved by dynamically changing the pitch angle of the individual blades and by keeping the wind speed of the tunnel constant. The blade loads are measured using strain gages and the flow velocity is measured upwind and downwind of the rotor using a hotwire. Dynamic inflow phenomena are clearly visible both in the turbine loads and in the velocity field. A time delay based upon the flow convection in the wake is identified. It results that the induction of the turbine can be controlled by changing the pitch of the blades. The experimental database allows to validate a new dynamic inflow model for VAWT and will be made publicly available for research purposes.

1. Introduction

Compared to the conventional horizontal-axis wind turbines (HAWTs), vertical-axis wind turbines (VAWTs) show advantages: among others the location of the centre of gravity closer to the ground makes VAWT a potentially better solution for offshore floating applications [1]; they are less noisy and suitable for the installation into urban environments [2]. However, the VAWT's performance is complex due to the 3D unsteady aerodynamics, such as dynamic stall, and the occurrence of structural effects. Additional complexities may be introduced by the motion of the floater or by a sudden change in the wind speed (i.e. gust). The consequent variation of the inflow wind velocity or the turbine loading cause dynamic inflow conditions at the rotor. This unsteady effect can be better investigated with scaled wind tunnel testing under controlled conditions.

2. Objective

The objective of this research is to experimentally replicate dynamic inflow conditions by changing the pitch angle of the individual blades. Dynamic inflow conditions are realised by dynamic thrust: a constant incoming wind and an unsteady change in the blade pitch angle (i.e. β). The consequent variations in the turbine loads and in the velocity field are studied. Hotwire flow measurements are used to quantify the velocity response for different pitch schedules by means of the time delay. The final outcome is a complete database allowing to validate dynamic inflow models for VAWTs.

3. Experimental setup

3.1. Wind tunnel and VAWT model

The experimental activity is carried out in the Open Jet Facility of Delft University of Technology, which is a low speed closed loop wind tunnel [3]. The test section is octagonal with an equivalent diameter of 3 m and a contraction ratio of 3:1. As a consequence, the stream results uniform with a turbulence intensity of 0.5 % up to 1 m from the nozzle exit and lower than 2% at 6 m from the nozzle [3]. The tunnel is powered by a 5×10^5 W fan and the flow velocity reaches its maximum at 34 m/s in the test section [3]. The tested model is a two-bladed H-Darrieus VAWT, referred to as PitchVAWT [4]. In order to minimize the deflection, two horizontal struts are used for each blade and located at approximately 25% and 75% of the blade length [5]. The turbine geometry, the experimental setup and the design specifications are shown in Figures 1 and 2 and Table 1, respectively. The turbine is provided with active individual blade pitch control. The pitch angle of each blade is controlled individually by the use of DC micromotors and positioning controllers. These controllers provide signal feedback to the turbine SCADA controller which, depending on the requested pitch scheme being tested, updates the pitch position of each blade. A set of sensors on the turbine allows to measure the azimuth position, the rotor torque, thrust load transferred to the tower base and normal blade loading. Data is collected using National Instruments^{TM} hardware at a sampling frequency of 5×10^2 Hz [4]. More detailed information about the design of the PitchVAWT can be found in a previous work [5].

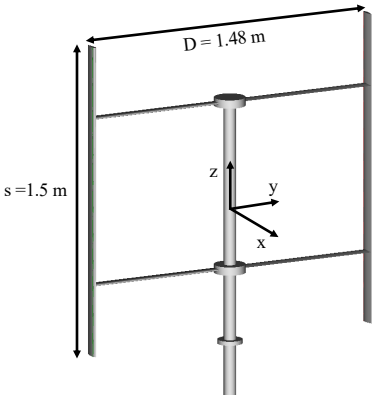

Figure 1. PitchVAWT geometry and dimensions.

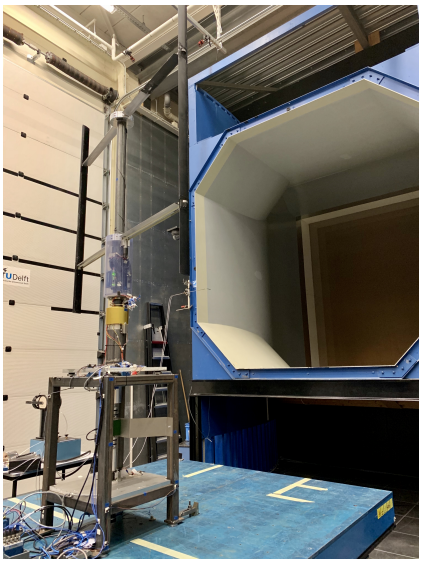

Figure 2. PitchVAWT installed in the Open Jet facility of Delft University of Technology.

3.2. Measurement techniques

During the experimental campaign, the wind speed of the tunnel was kept constant at 4 m/s while the PitchVAWT was operating at different rotational speeds (i.e. 52 rpm, 77 rpm, 103 rpm, 129 rpm, 155 rpm, 181 rpm and 206 rpm). Due to the high angles of attack and as a consequence severe stall characteristics experienced by the turbine at low tip speed ratios (TSRs), only TSRs 3 and 4 are analysed further. Instantaneous measurements of the flow velocity at several locations upwind and downwind of the rotor are performed using hotwire

Table 1. PitchVAWT design specifications [5].

Parameter	Value
Number of blades (N_b)	2
Span (s)	1.5 m
Diameter (D)	1.5 m
Chord (c)	7.5×10^{-2} m
Solidity (σ)	0.1
Blade airfoil	NACA0021
Strut airfoil	NACA0018

at a sampling frequency of 1.6×10^3 Hz. The hotwire structure can move along the x-y plane while the height is fixed at the mid-rotor plane to approach 2D conditions and to avoid the strut interference as much as possible. Figure 3 illustrates the experimental setup: A and B identify the hotwire system and the VAWT, respectively. Figure 4 depicts the hotwire measurement grid and the system of reference adopted in the discussion of the results. The blade orbit is divided in 2 regions: upwind, $0° < \theta < 180°$, and downwind, $180° < \theta < 360°$, with θ being the blade azimuthal positions. θ is defined with respect to blade 1, therefore blade 2 lags blade 1 by 180°. The coordinate system is a Cartesian frame with the origin at the turbine center; the x-axis is directed in inflow direction, the y-axis in crossflow direction and the z-axis in spanwise direction.

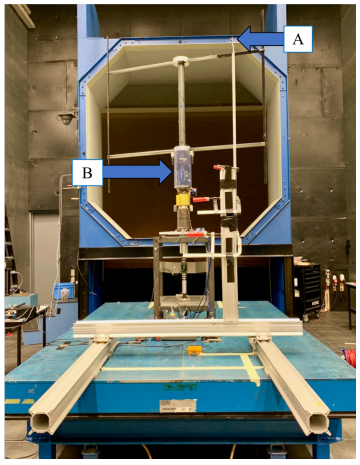

Figure 3. Experimental setup for the hotwire (A) in the Open Jet Facility at Delft University of Technology. (B) indicates the VAWT.

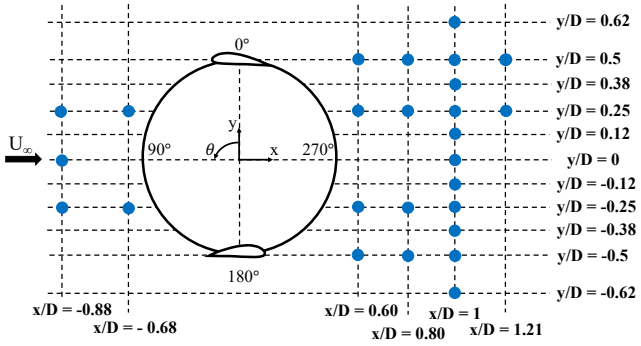

Figure 4. Hotwire measurement grid. The measurement points are coloured in blue. The coordinate system for the turbine is shown in the center.

3.3. Pitch cases and expected load cases

To create a reliable database, three different load cases are studied:

(i) a step input in blade forces created by a constant pitch angle on both blades (Equation (1));

(ii) a step input in thrust generated with a sinusoidal pitch, depending on the azimuth angle of each individual blade (Equation (2));

(iii) a cyclic thrust generated by a multi-sinusoidal pitch schedule (Equation (3)).

$$\beta = \beta_0, \tag{1}$$

$$\beta = A\sin(\theta), \tag{2}$$

$$\beta = A\sin(\theta)\sin(N_{rot}\,\theta). \tag{3}$$

where β_0 is the baseline pitch and N_{rot} is the number of rotations after which the same pitch schedule is repeated. To clarify the expected effects of these pitch schedules, the results of the steady Actuator Cylinder model [6] are presented in Figures 5 to 9. A constant pitch angle is independent of the azimuthal position. Its effect is to redistribute the loads between the upwind and the downwind half, as is illustrated in Figures 5 and 6. A constant pitch of 5° is applied after 3.5 turbine rotations leading to a step increase in the angle of attack of blade 1 and thus in the force. By looking at the consequent response of the thrust at the rotor (Figure 7), it is clear that the effect of the change in pitch is compensanted by the two blades and no significant change in the overall thrust can be recognized. In case of the sinusoidal pitch, it is different. Since the resulting pitch now depends on the azimuth angle (i.e. θ), its frequency corresponds to the rotational frequency of the turbine (i.e. f_{rot}). The pitch angle now is different for every azimuthal position but it will be the same every single rotation. Consequently, the thrust at the turbine rotor is expected to show a step input when this pitch schedule is activated. This effect can be seen in Figure 8. The turbine thrust responds to a sinusoidal pitch ($A = 7$) with a step increase. When the pitch schedule is prescribed by a multi-sinusoidal equation, a second frequency is recognised as a function of the number of rotation (i.e. N_{rot}). The pitch angle will change for every azimuthal position and rotation. The same pitch schedule is only repeated after N_{rot} rotations. Thus, it is expected to have a sinusoidal variation in the thrust with a second frequency on top of the standard sinusoidal variation with respect to the turbine rotational frequency. This is confirmed by the results in Figure 9. Here, the thrust is cyclically varying every 5 rotation ($N_{rot} = 5$) due to a multi-sinusoidal pitch of $A = 5$. A summary of the pitch schedules tested during the experimental campaign is provided in Table 2.

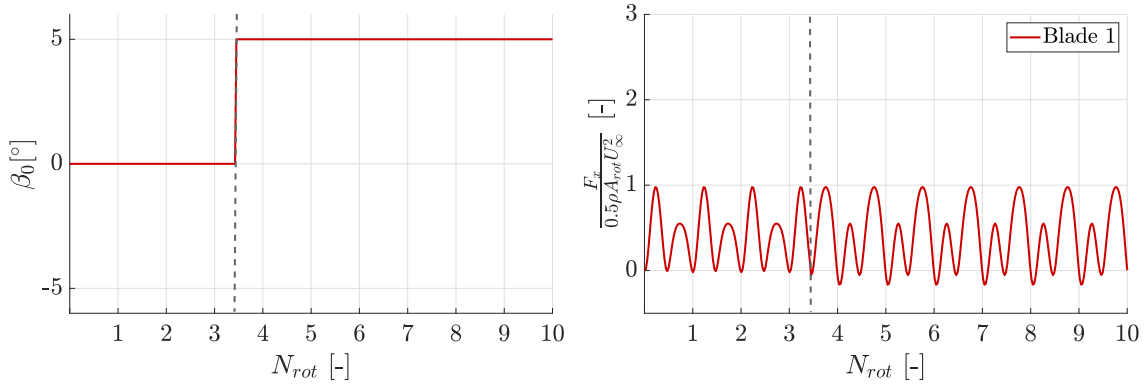

Figure 5. Simulation of the response of the non-dimensional force on blade 1 to a constant pitch schedule ($\beta = \beta_0$ with $\beta_0 = 5°$). The results are obtained with the steady Actuator Cylinder model [6].

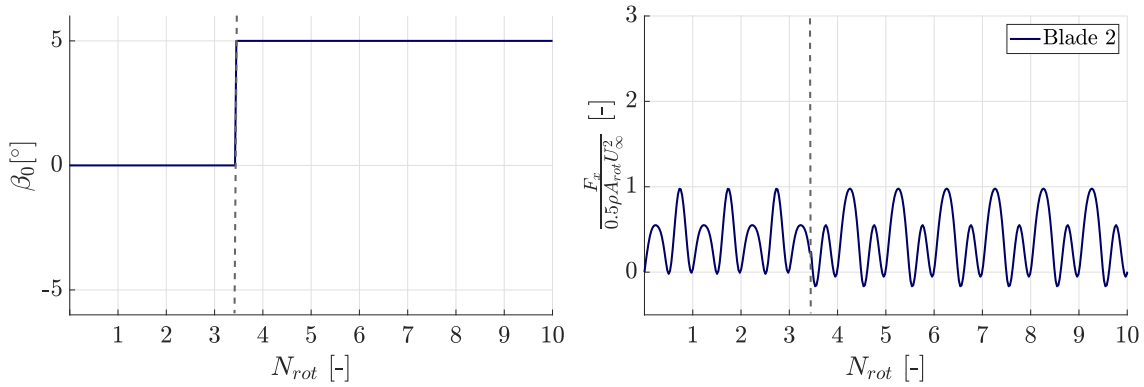

Figure 6. Simulation of the response of the non-dimensional force on blade 2 to a constant pitch schedule ($\beta = \beta_0$ with $\beta_0 = 5°$). The results are obtained with the steady Actuator Cylinder model [6].

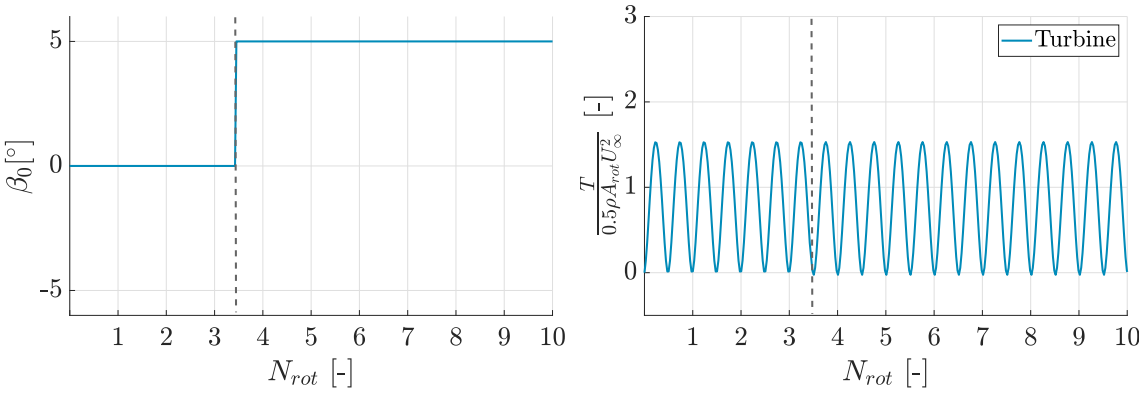

Figure 7. Simulation of the non-dimensional thrust response to a constant pitch schedule ($\beta = \beta_0$ with $\beta_0 = 5°$). The results are obtained with the steady Actuator Cylinder model [6].

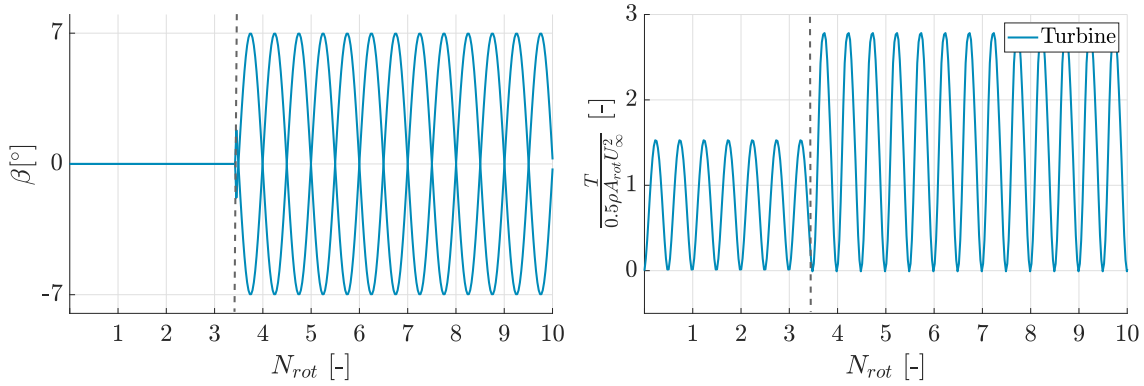

Figure 8. Simulation of the non-dimensional thrust response to a positive sinusoidal pitch schedule ($\beta = A\sin(\theta)$ with $A = 7$). The results are obtained with the steady Actuator Cylinder model [6].

3.4. Calculation of thrust loads

The normal blade load ($F_{n_{blade}}$) is measured using a set of strain gages on the top strut of blade 1. Due to the symmetrical design of the blades and struts, the assumption is made that the

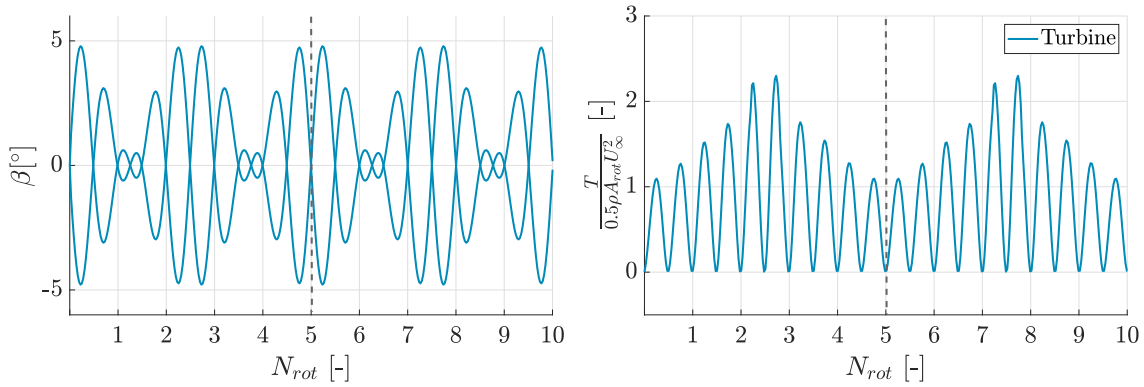

Figure 9. Simulation of the non-dimensional thrust response to a multi-sinusoidal pitch schedule ($\beta = A\sin(\theta)\sin(N_{rot}\theta)$ with $A = 5$ and $N_{rot} = 5$). The results are obtained with the steady Actuator Cylinder model [6].

Table 2. Pitch schedules tested during the experimental campaign.

Type	β_0	A	N_{rot}
Constant	3, -3, 5, -5	-	-
Sinusoidal	-	-7,-5,-3, 3, 5, 7	-
Multi-sinusoidal	-	3	1, 2, 3, 4, 5, 6
	-	5	1, 2, 3, 4, 5, 6
	-	7	1, 2

normal loading is equally distributed among the struts and that both struts are transferring the same amount of blade loads. Also a symmetry between both blades is assumed. The time signal of the normal load contains a large amount of high frequency noise which is the result of the testing environment and wiring. The maximum turbine operational frequency is approximately 4 Hz. Since there are no relevant phenomena occuring above ten times this value, a low pass filter is applied to the data at 45 Hz. Using the structural model developed in [7], the following modes are identified and filtered from the measured $F_{n_{blade}}$, as they do not contribute to the aerodynamic loading:

- the tower backwards whirl mode (10.4 Hz),
- the tower forward whirl mode (17.8 Hz),
- the blade edgewise in-phase mode (20.3 Hz),
- the blade edgewise out-phase mode (20.8 Hz),
- the platform torsional mode (21.3 Hz).

The final step in the post-processing of the normal load measurement data is the removal of the centrifugal force. This significantly large load corresponds to a suspended mass having an acceleration proportional to the square of the rotational frequency. For a point mass, the centrifugal load is simplified to $F_{cent} = mr\omega^2$. However, for the VAWT, the phenomenon is much more complex and therefore a second order correction model is derived from the normal load measured at various rotational frequencies in absence of incoming wind. This accounts for any non-linearity built into the system, as well as the exact spring mass outboard of the

strain gage placement. By knowing the normal load, the force on blade 1 is calculated with Equation (4). It is important to notice that the tangential load ($F_{t_{blade}}$) is not measured in this experiment but its contribution is assumed to be very small. Since the design of the VAWT is symmetric, the force on blade 2 can be obtained by phase-shifting the force on blade 1. The thrust of the entire turbine (T) is then determined by summing the contributions of the forces on the two blades.

$$F_x \simeq F_{n_{blade}} \sin(\theta). \tag{4}$$

4. Results

4.1. Turbine loads

In the following section, the experimental thrust variation over one turbine revolution (T), the thrust coefficient (C_T), i.e. the normalised thrust averaged over one rotation, and the average thrust (T_{avg}), i.e. the thrust variation smoothed using the moving average method, are analysed. These variables are non-dimensionalized with respect to $0.5\rho A_{rot} U_\infty^2$. Figure 10 shows the experimental T and the corresponding C_T for different constant pitch angles: $-5°$, $-3°$, $0°$, $3°$ and $5°$. Data is taken at a TSR of 4, binned into 360 segments of 1 degree and averaged over 40 rotations. Since the loads of the VAWT vary considerably during one rotation, it is necessary to present the data in the azimuthal domain to assess the aerodynamic performance of the turbine. A maximum thrust can be recognized at around $\theta = 90°$, where blade 1 is upwind, and at $\theta = 270°$, where blade 2 is upwind. These peaks correspond to the expected maximum loadings. By looking at the trend of C_T, it may be observed that C_T starts to decrease with increasing pitch angle, after it reached its maximum at $\beta_0 = -3°$. In inviscid conditions, the effect of a constant pitch angle would only cause a redistribution of the loads between the upper and lower half of the rotor, and thus no effect will be observed in the overall thrust (as was the case for the AC results in Section 3.3). However, since the experiment is viscid and the blades do operate near or even in stalled conditions depending on the pitch angle, there is an optimal pitch angle. As a consequence, a change in thurst is noticeable for different constant pitch schedules. The experimental T and the corresponding C_T are also computed for different sinusoidal pitch schedules with A = -7, A = -5, A = -3, $A = 0$, $A = 3$, $A = 5$, $A = 7$. The results are illustrated in Figure 11 for a TSR of 4. With respect to the constant case, an opposite trend for the C_T can be recognized here. The C_T increases for positive pitch angles. A positive A value makes the angle of attack larger upwind and more negative downwind. A negative A indicates a decreased angle of attack upwind and a less negative angle downwind. The responses of T_{avg} to a sinusoidal pitch schedule and to a multi-sinusoidal pitch schedule are plotted in Figures 12 and 13, respectively. The moving average method is performed over the experimental measurements to minimise the effect of external perturbations. When the sinusoidal pitch is activated after two revolutions ($N_{rot} = 2$), the thrust responds only after three revolutions ($N_{rot} = 3$) and it stabilizes only at the 6th revolution ($N_{rot} = 6$). This confirms that the change in the pitch angle causes a change in the turbine load. Furthermore, this load variation does not occur instantaneously but with a gradual change and thus a delay in time. The sinusoidal variation in thrust due to a multi-sinusoidal pitch is also confirmed. It can be observed that the thrust is cyclically changing with a second frequency corresponding to 5 f_{rot}, which corresponds to the rate of change of the implemented pitch schedule.

4.2. Flow field

The variable load achieved with a variable pitch schedule causes a change in the velocity field. This change does not occur instantaneously but gradually from one equilibrium to another. In order to quantify this effect, the time delay between the activation of the sinusoidal pitch and the response of the velocity field in the point $(x/D, y/D) = (0.80, 0.25)$ is computed for two different TSRs (i.e. 3 and 4). Figure 14 confirms that the time delay is higher for a heavily

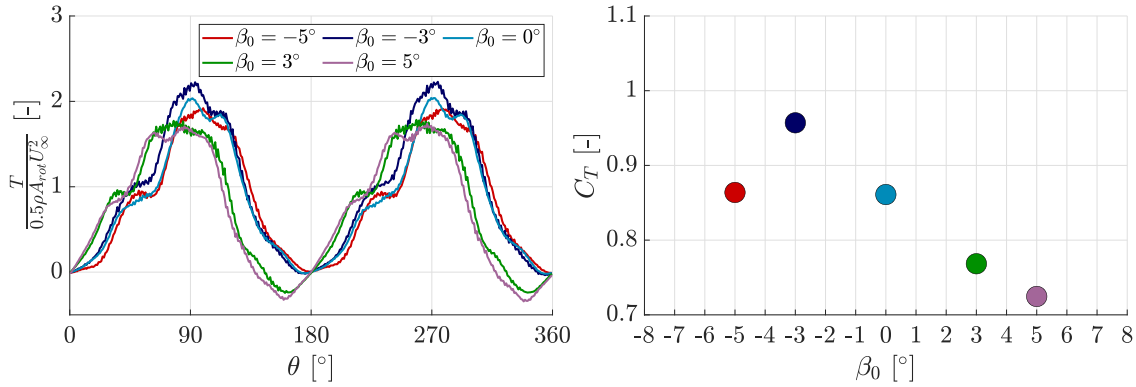

Figure 10. Experimental non-dimensional thrust of the turbine (T) over one turbine revolution (left-side) and corresponding thrust coefficient (C_T) (right-side) for different constant pitch:$-5°$, $-3°$, $0°$, $3°$ and $5°$ ($\beta = \beta_0$).

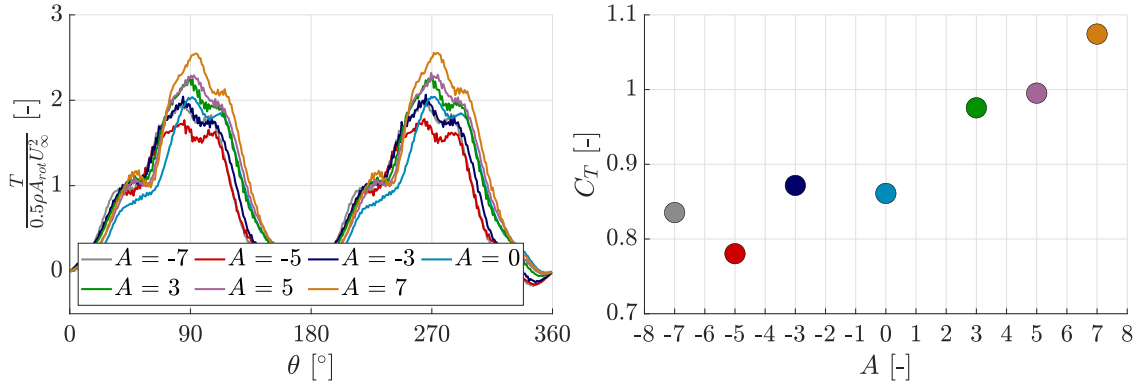

Figure 11. Experimental non-dimensional thrust of the turbine (T) over one turbine revolution (left-side) and corresponding thrust coefficient (C_T) (right-side) for different sinusoidal pitch schedules: $\beta = A\sin(\theta)$ with $A = -7$,$A = -5$, $A = -3$, $A = 0$, $A = 3$, $A = 5$, $A = 7$.

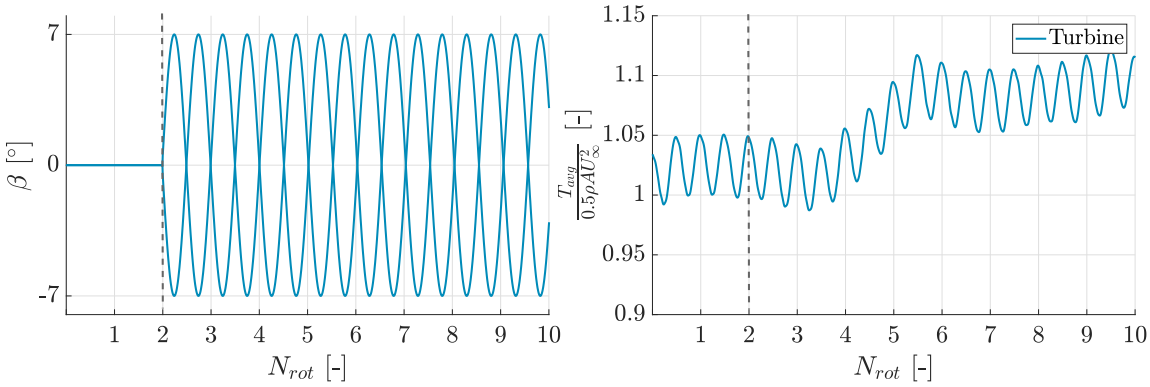

Figure 12. Experimental step input in thrust due to a sinusoidal pitch schedule ($\beta = A\sin(\theta)$ with $A = 7$).

loaded rotor (i.e. TSR 4) and lower for a lightly loaded rotor. This is due to the different wake velocities, which are initially slower for heavier loaded case and faster for the lighter loaded case.

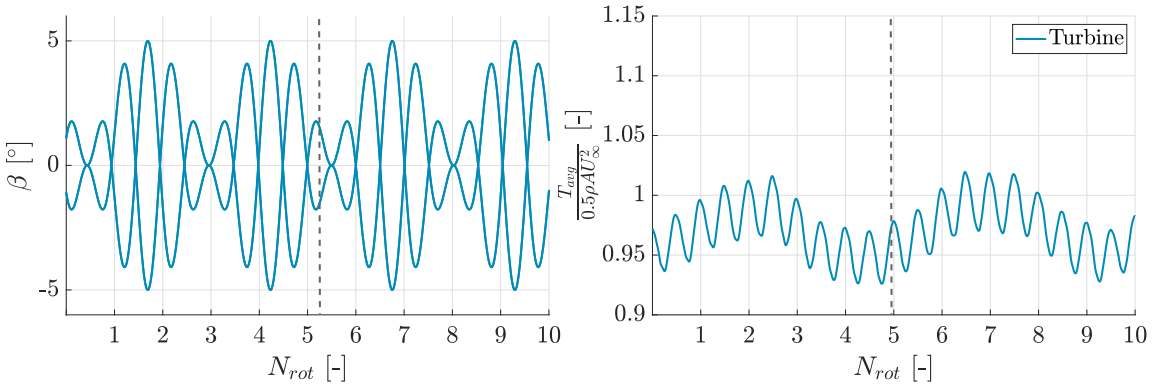

Figure 13. Experimental cyclic thrust due to a multi-sinusoidal pitch schedule ($\beta = A\sin(\theta)\sin(N_{rot}\theta)$ with $A = 5$ and $N_{rot} = 5$).

Figures 15 and 16 depict how the x-velocity in the wake, U_w, responds to a multi-sinusoidal pitch schedule ($A = 5$ and $N_{rot} = 5$). For both cases, the U_w changes cyclically every five rotations with the same trend of the turbine load (Figure 13). In Figure 15, three points with the same y/D coordinate and different x/D coordinates are considered: $(x/D, y/D) = (0.60,-0.25)$, $(x/D, y/D) = (0.80,-0.25)$, $(x/D, y/D) = (1,-0.25)$. As it is expected, U_w decreases when moving downstream [8]. For Figure 16, the same X coordinate is chosen and the y/D coordinate varies between -0.50 and 0.50. At $(x/D, y/D) = (0.80,0.50)$ and $(x/D, y/D) = (0.80,-0.50)$, U_w is double with respect to the velocity measured in $(x/D, y/D) = (0.80,0.25)$ and in $(x/D, y/D) = (0.80,-0.25)$. This is because, these two extreme approximately represent the edges of the wake, where the velocity is close to the free-stream velocity (i.e. 4 m/s). However, the highest U_w is measured at $(x/D, y/D) = (0.80,0.50)$ because the wake in the VAWT is sligthly asymmetric [8].

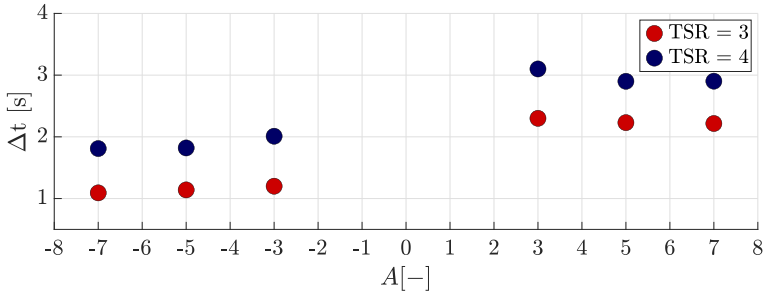

Figure 14. Experimental time delay between the activation of the sinusoidal pitch and the response of the velocity field. Two different tip speed ratios (i.e. TSRs) are analyzed: 3 (in red) and 4 (in blue). The velocity field is measured in the point $(x/D,y/D) = (0.80,0.25)$.

5. Conclusions

This study presents an experimental campaign of applying variable loads on a VAWT by means of individual blade pitching. The response of the turbine thrust force to various pitch schedules is shown to be in line with analytical results of the AC model. When changing the pitch schedule from one to another, the turbine thrust measurements indicated a lag in its response. A similar delay is identified in the velocity measured in the wake. This phenomenon confirms that variable blade pitching can be used to demonstrate dynamic inflow conditions. This study provides an

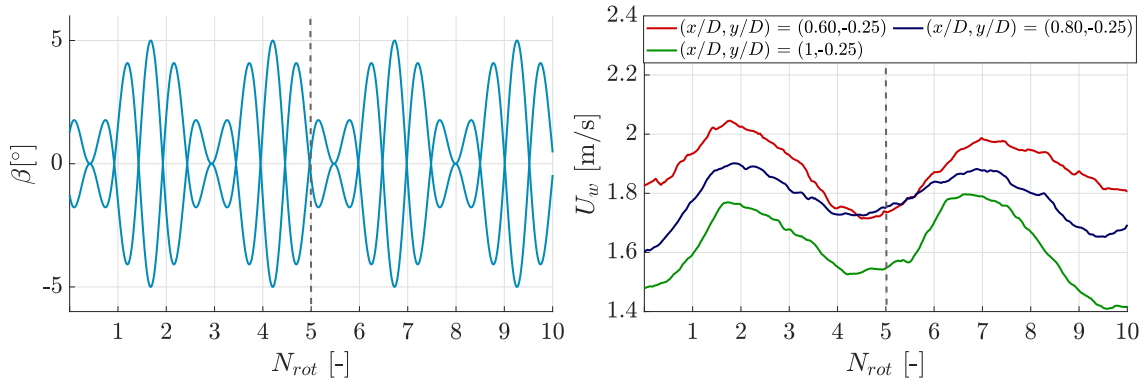

Figure 15. Experimental response of the x-velocity in the wake U_w in three points downstream due to a multi-sinusoidal pitch schedule ($\beta = A\sin(\theta)\sin(N_{rot}\theta)$ with $A = 5$ and $N_{rot} = 5$).

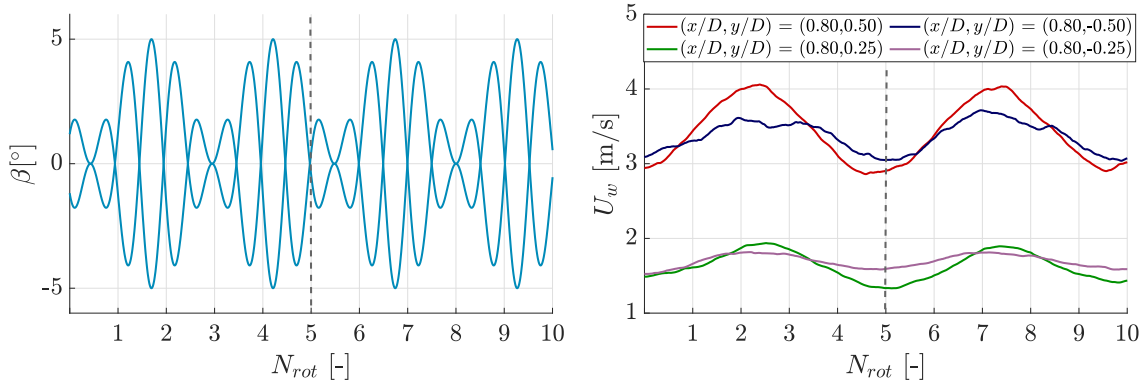

Figure 16. Experimental response of the x-velocity in the wake U_w in four points downstream due to a multi-sinusoidal pitch schedule ($\beta = A\sin(\theta)\sin(N_{rot}\theta)$ with $A = 5$ and $N_{rot} = 5$).

extensive experimental database that may be used to validate dynamic inflow models for VAWTs. The data will be made publicly available for research purposes.

Acknowledgments

This research is part of the Arkom-Tulyp Wind project and is sponsored by RVO, the Netherlands Enterprise Agency, under a Hernieuwbare Energie (Sustainable Energy) subsidy.

References

[1] Eriksson S, Bernhoff H, Leijon M 2008 Evaluation of different turbine concepts for wind power *Renewable Sustainable Energy Revision* **12** 1419-1434.
[2] Möllerström E, Ottermo F, Hylander J, Bernhoff H, 2016 Noise emission of a 200 kW vertical-axis wind turbine *Energies* **19** 1-10.
[3] Lignarolo L E M, Ragni D, Krishnaswani C, Chen Q, Ferreira C, van Bussel G J W, 2014 Experimental analysis of the wake of a horizontal-axis wind-turbine model *Renewable Energy* **70** 31–46.
[4] LeBlanc B and Ferreira C 2018 Experimental determination of thrust loading of a 2-bladed vertical axis wind turbine *J. Phys. Conf. Ser* **1037** 2.
[5] LeBlanc B and Ferreira C 2018 Overview and design of PitchVAWT: vertical axis wind turbine with active variable pitch for experimental and numerical comparison *AIAA* **2018-1243** https://doi.org/10.2514/6.2018-1243.
[6] Madsen H 1982 The Actuator Cylinder - a flow model for vertical axis wind turbines *Aalborg University Centre report* ISBN 87-87681-04-8 https://doi.org/10.13140/RG.2.1.2512.3040.

[7] LeBlanc B and Ferreira C 2019 Experimental characterization of H-VAWT turbine for development of a digital twin *NAWEA Conf.* In-printed.
[8] Tescione G, Ragni D, He C, Ferreira C, van Bussel G J W, 2014 Near wake flow analysis of a vertical axis wind turbine by stereoscopic particle image velocimetry *Renewable Energy* **70** 47-61.